IOPscience iopscience.iop.org

Home Search Collections Journals About Contact us My IOPscience

Modelling a spin-selective interface between ferromagnetic electrodes and a carbon nanotube—towards the enhanced giant magnetoresistance effect

This article has been downloaded from IOPscience. Please scroll down to see the full text article.

2004 J. Phys.: Condens. Matter 16 2981

(http://iopscience.iop.org/0953-8984/16/17/025)

View the table of contents for this issue, or go to the journal homepage for more

Download details:
IP Address: 129.252.86.83
The article was downloaded on 27/05/2010 at 14:33

Please note that terms and conditions apply.

INSTITUTE OF PHYSICS PUBLISHING JOURNAL OF PHYSICS: CONDENSED MATTER

J. Phys.: Condens. Matter **16** (2004) 2981–2989 PII: S0953-8984(04)69899-7

Modelling a spin-selective interface between ferromagnetic electrodes and a carbon nanotube—towards the enhanced giant magnetoresistance effect

S Krompiewski

Institute of Molecular Physics, Polish Academy of Sciences, ulica M Smoluchowskiego 17, 60-179 Poznań, Poland

Received 2 October 2003
Published 16 April 2004
Online at stacks.iop.org/JPhysCM/16/2981
DOI: 10.1088/0953-8984/16/17/025

Abstract

The effect of interface conditions on the giant magnetoresistance (GMR) is studied. It is shown that the GMR changes drastically in the presence of extra magnetic monolayers at the ferromagnetic electrodes. The monolayers may make the spin-dependent conductance channels nearly or completely closed if they are antiferromagnetically exchange coupled to the electrodes. It is shown that the conductance spectrum of the device reflects, to a large degree, the internal band structure of the nanotube. Therefore the GMR effect is quite sensitive to the relative bands' line-up of electrodes and the nanotube and it may be tuned by a gate voltage applied to the nanotube.

(Some figures in this article are in colour only in the electronic version)

1. Introduction

Recently there has been growing interest in electronic transport through molecular systems (see [1–3]). This is motivated by the future electronics requirements concerning miniaturization. In particular it is predicted that in ten years or so the silicon-based technology will face a barrier of fundamental nature [4]. Out of many possible molecular systems carbon nanotubes have been attracting particular attention due to their exceptional mechanical and electrical properties (see [5, 6]). Recently, attempts have been made to study spin-dependent transport through carbon nanotubes sandwiched between ferromagnetic electrodes. The experimental papers deal mostly with multi-wall carbon nanotubes (MWCNT) and produce results which differ very much not only quantitatively but also qualitatively from one another. Reported maximum GMR values range from 9% [7] (Co contacts), through 30% [8] (Co contacts), up to 100% [9] (Fe contacts). By qualitative differences we mean in this context, on the one hand, the occurrence of the so-called inverse GMR, found in some samples in [8], and

 © 2004 IOP Publishing Ltd Printed in the UK

in permalloy contacted MWCNT in [10] with GMR $= -35\%$, while, on the other hand, the complete blockade of electron transport in the case of anti-aligned ferromagnetic electrodes, as reported in [9]. Theoretical papers devoted to the problem under consideration are scarce (see [11–13]).

So far the electrodes have been modelled as ideal homogeneous slabs (semi-infinite lead wires) without paying much attention to their surface magnetism. It is, however, well known that surface magnetic moments are usually either 'naturally' enhanced with respect to the bulk values due to the reduced neighbourhood or drastically modified if the surface is oxidized. 3d transition metal monoxides are antiferromagnets, crystallizing in the rocksalt structure, with parallelly oriented magnetic moments in the same (111) crystallographic plane. The magnetic moments are then even more enhanced and equal to 1.77 μ_B, 3.35 μ_B and 3.32 μ_B for NiO, CoO and FeO, respectively [14] (to be compared with 0.6, 1.7 and 2.2 for pure Ni, Co and Fe). The aim of this paper is to show what the influence of the extra magnetic monolayer at the electrode is, and to test under what circumstances it can lead to a strong suppression of spin-dependent transport channels. This study makes it possible to gain a qualitative insight into the simplest physical mechanism which may account for the aforementioned extraordinary spin selectivity.

2. Methodology

We adopt the standard single-band tight-binding Hamiltonian to describe π and s electrons in the single wall carbon nanotube (SWCNT) and ferromagnetic electrodes, respectively. The on-site potentials in the SWCNT are initially set to 0, whereas in the electrodes and in the monolayers they are spin-dependent and chosen so as to give a required magnetization (see below). Within the Green function formalism we exploit the following relations, using the standard notation (cf [15]):

$$H = \sum_{i,j,\sigma} t_{i,j}|\sigma,i\rangle\langle j,\sigma| + \sum_{i,\sigma}\epsilon_{i,\sigma}|\sigma,i\rangle\langle i,\sigma|, \tag{1}$$

$$\begin{pmatrix} E_\sigma - H_L^\sigma & V_{LC} & 0 \\ V_{LC}^\dagger & E_\sigma - H_C^\sigma & V_{CR} \\ 0 & V_{CR}^\dagger & E_\sigma - H_R^\sigma \end{pmatrix} \hat{\mathcal{G}}_\sigma = \hat{1}, \tag{2}$$

$$G_\sigma \equiv \hat{\mathcal{G}}_C^\sigma = (\hat{1}E_\sigma - H_C^\sigma - \Sigma_{L,\sigma} - \Sigma_{R,\sigma})^{-1}, \tag{3}$$

$$n_\sigma = \frac{1}{2\pi}\int \mathrm{d}E\, G_\sigma(f_{L,\sigma}\Gamma_{L,\sigma} + f_{R,\sigma}\Gamma_{R,\sigma})G_\sigma^\dagger, \tag{4}$$

$$I_\sigma = \frac{e}{h}\int_{-\infty}^{\infty}\mathrm{d}E(f_{L,\sigma} - f_{R,\sigma})\,\mathrm{Tr}[\Gamma_{L,\sigma}G_\sigma\Gamma_{R,\sigma}G_\sigma^\dagger], \tag{5}$$

where

$$\Gamma_{\alpha,\sigma} = \mathrm{i}(\Sigma_{\alpha,\sigma} - \Sigma_{\alpha,\sigma}^\dagger), \qquad \Sigma_{\alpha,\sigma} = V_{C,\alpha}g_{\alpha,\sigma}V_{C,\alpha}^\dagger \qquad f_{\alpha,\sigma} = \left(1 + \exp\left[\frac{E_\sigma - \mu_\alpha}{k_B T}\right]\right)^{-1}$$

and $\alpha = $ L, R stand for left- and right-hand sides, σ denotes the spin and the chemical potentials μ_α contain the voltage shifts. The Green function problem is solved by the partitioning technique (equation (2)) with H_C describing the central part of the device, H_α describing the electrodes and $V_{\alpha C}$ the corresponding coupling matrices. Moreover, t_{ij} are hopping integrals, ϵ are on-site potentials, n is the electron density matrix, I is the current and g_α is the αth electrode Green function. The spin dependence enters equations (1)–(5) via the on-site energies ϵ_i which depend on spin unless i refers to a carbon atom.

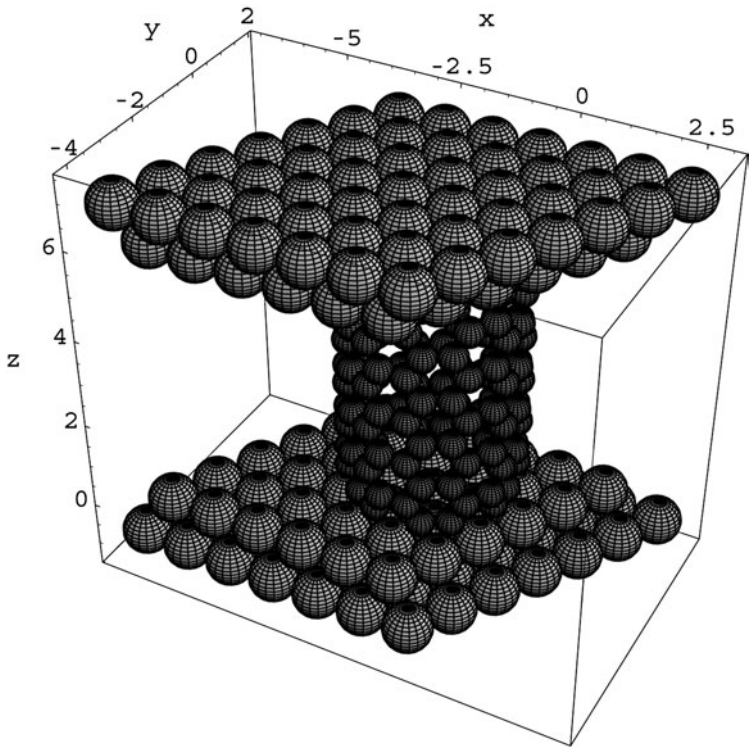

Figure 1. Schematic of the device. The outermost 7×7 atom planes belong to the ferromagnetic electrodes (infinite in all three directions). The 6×6 atom planes represent an extra monolayer ('transition metal oxide atoms'), whereas the SWCNT is represented by small spheres.

3. Modelling and results

3.1. Structural models

The modelling of the structures studied proceeds as follows:

- The electrodes are modelled as semi-infinite metallic slabs of fcc (111) crystallographic structure. The slabs are also infinite in the transverse (to the current) directions and are composed of 3d transition atoms represented by dense packed large spheres of diameter 1 (in the armchair lattice constant units, $a = 2.49$ Å).
- The outermost atomic plane of the left (right) electrode is finite and contains 49 atoms. These planes will be formally included in the so-called extended molecule in order to meet a charge neutrality requirement.
- The extra magnetic monolayer is constructed likewise, but this time the layer is a bit smaller and consists of just 36 atoms—forming a sort of a neck.
- Between the left monolayer and the right one is placed the armchair SWCNT, with a wrapping vector (m, n), $m = n = 6$. It is modelled by means of small spheres ($1/\sqrt{3}$ in diameter) representing carbon atoms. The nanotube is perfectly contacted with magnetic monolayers, i.e. each interface carbon atom has got exactly three neighbours in the adjacent monolayer (see figure 1).

For the (6, 6) chiral vector this construction is possible if the interface carbon-ring diameters are slightly (a few per cent) smaller than those of the other rings with a standard perimeter of $m\sqrt{3}$. Of course, for an arbitrary wrapping vector the matching is no longer so good and one must redefine the hopping integral range by making the t parameters distance-dependent. Henceforth the SWCNT, together with the two finite adjacent monolayers at each end, will be referred to as an extended molecule and described by the Hamiltonian H_{C}.

3.2. Details of calculations

Detailed computations presented below are carried out for symmetric structures with armchair SWCNTs of length equal to $L = 20.5$ lattice constant units (41 carbon rings). Due to the quite exceptional low-energy spectrum of the armchair SWCNT the characteristic features of the conductance spectra for other lengths may be predicted on scaling the energy axis by the factor $1/L$ (because the average inter-peak distance goes roughly as $\hbar v_{\mathrm{F}}/L$, see, e.g., [16]).

The Green function of the semi-infinite electrodes have been calculated analytically as in [17] and the summation over the two-dimensional Brillouin zone has been performed by the *special k-points-method* [18]. The zero bias conductance has been calculated from equation (5) and used to define the giant magnetoresistance as either $\mathrm{GMR} = 100(1 - G_{\uparrow\uparrow\downarrow\downarrow}/G_{\uparrow\uparrow\uparrow\uparrow})$ or $100(1 - G_{\uparrow\downarrow\uparrow\downarrow}/G_{\uparrow\uparrow\uparrow\uparrow})$, where $G = (\mathrm{d}I/\mathrm{d}V)_{V=0}$ denotes the conductance and the outer arrows refer to aligned and anti-aligned ferromagnetic electrodes, whereas the inner ones refer to the extra magnetic monolayers at the interfaces. Hereafter, in order to avoid confusion, the orientation of the electrode magnetization with respect to the adjacent extra magnetic monolayer will be referred to as being due to either ferromagnetic or antiferromagnetic coupling, whereas the relative orientations of external electrodes to each other will be described as either parallel or antiparallel alignments (configurations). The coupling and the alignment (of the electrodes) are assumed to be independent of each other. While parametrizing the Hamiltonian we have chosen the polarization of the electrodes to be 50% with $\epsilon_{\uparrow} = -2.32$ and $\epsilon_{\downarrow} = 1.6$ (the number of electrons being 0.75 and 0.25 for majority and minority bands, respectively). The magnetic moment per atom in the additional magnetic monolayer has been assumed either to have the same on-site potential or a larger Stoner splitting with $\epsilon_{\uparrow} = -2.93$ and $\epsilon_{\downarrow} = 3.86$ (nominal magnetization 75%). To flip the spin direction the following interchange has been made: $\epsilon_{\uparrow} \Longleftrightarrow \epsilon_{\downarrow}$. The reference value of the hopping integral is $t = -1$ and it is allowed to deviate from this value and take an arbitrary value t_{c} only for hoppings between the finite atomic planes outside the SWCNT. In what follows we shall put t_{c} equal to either -1 or -0.35. The latter value was deduced on the basis of [19] (where the exchange integral between CoO and Co magnetic moments is estimated) by assuming that exchange integrals scale as t^2, as in the well-known t/U Hubbard model expansion.

Conductance of a molecule coupled to the external electrodes depends critically on the position of the Fermi energy, the strength of the coupling and the internal structure of the molecule [20]. While the third factor is treated exactly within the present simple model, the first two need commenting upon. The coupling in the present case is determined by the perfect geometrical contacting of particular segments of the device (see figure 1) and all hopping parameters are set to -1, except that between the electrode's outermost finite (49 atoms) plane and the extra 'oxide monolayer' (t_{c}). The interface magnetic monolayers as well as the finite atomic planes of the electrodes are incorporated into the molecule (extended molecule concept). To make an energy band line-up, all the on-site potentials within the extended molecule are self-consistently shifted so as to guarantee the global charge neutrality.

In the case of SWCNTs supported on Au(111) the consensus has been gained that the Fermi level is shifted towards lower energies by $\delta E \sim 0.3$ eV with respect to E_{F} of a decoupled

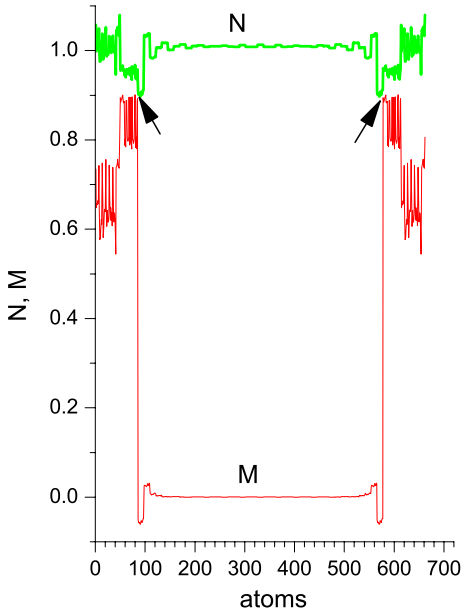

Figure 2. Numbers of electrons per atom ($N = N^{\uparrow} + N^{\downarrow}$) and the respective magnetic moments ($M = N^{\uparrow} - N^{\downarrow}$) for the parallel aligned electrodes, ferromagnetically coupled to the monolayers. The first (last) 49 atoms belong to the source (drain) ferromagnetic electrodes. Next the extra monolayers come (36 atoms each) and in the middle there are 41 carbon rings (each ring contains 12 atoms). The arrows indicate the electron deficiency regions at the ends of the SWCNT. The parameters are: $\epsilon_{\text{electrode}\uparrow} = -2.32$, $\epsilon_{\text{electrode}\downarrow} = 1.6$, $\epsilon_{\text{mono}\uparrow} = -2.93$, $\epsilon_{\text{mono}\downarrow} = 3.86$ and $t_c = -1$.

nanotube. The shift is due to the difference in work functions of gold and nanotubes (5.3 and 4.3 eV, respectively) and results in some charge transfer from the SWCNT to Au. The direct way to measure this effect is scanning tunnelling spectroscopy, which yields differential conductance and allows us to estimate δE either from the asymmetry of the conductance spectra (see [21, 22]) or from spectacular beating patterns of $\mathrm{d}I/\mathrm{d}V$ oscillatory length scans [23]. Of course, the STS experiment probes transport in the direction perpendicular to the nanotube axis, whereas in our theory transport occurs along the nanotube axis. Nevertheless, the band line-up adopted by us also leads to the electron deficiency in the ends of the SWCNT (see figure 2). Moreover the figure shows that: (i) at the interface the carbon atoms get spin-polarized, (ii) the number of electrons slightly fluctuates within a ring (quasi-plateaux) and (iii) the interface effects are pronounced up to the distance of 5–6 carbon rings away from the interface.

3.3. Discussion

At the first stage of our electron transport studies we have considered the simple case when the extra magnetic monolayer has the same spin polarization as the electrode and is ferromagnetically coupled to it. As is readily seen from figure 3, the conductances at the Fermi energy $E_F = 0$ are quite high in this case (the maximum theoretical value for the ideal SWCNT would be $4e^2/h$). Also the GMR effect is roughly Julliere-like, i.e. close to $2P^2/(1 + P^2)$. In the case when the electrode and the monolayer are antiferromagnetically oriented to each other the conductance becomes considerably reduced, resulting in an increase in GMR (figure 4). Figure 5, in turn, illustrates the case which in the present model mimics the situation with a

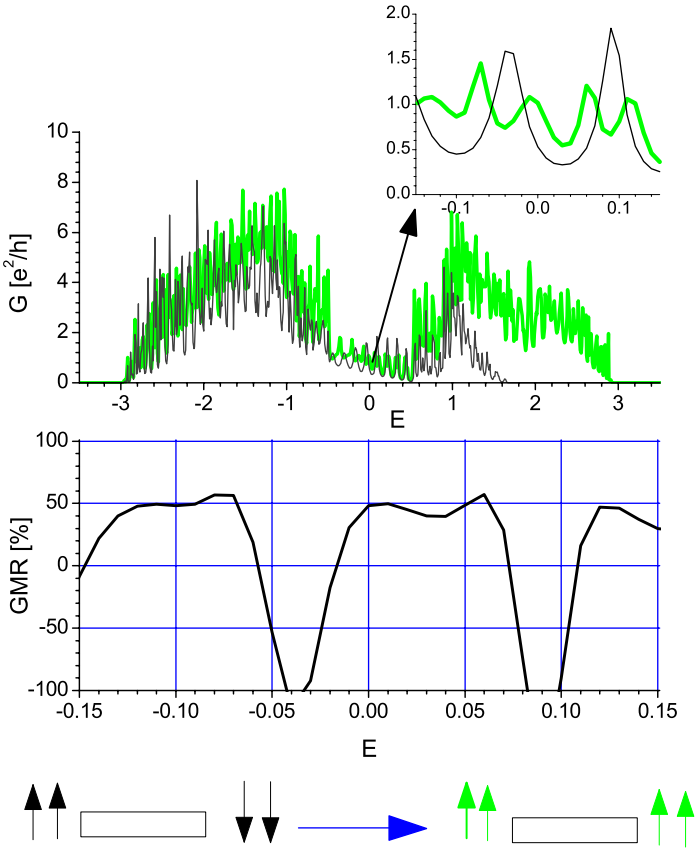

Figure 3. Extra magnetic layer with spin polarization 50% is ferromagnetically coupled to the magnetic electrode with the same nominal polarization and the hopping parameter $t_c = -1$. Conductance, G, in the parallel (thick curve) and in the antiparallel (thin curve) configurations, and GMR (bottom panel). The inset shows G in the vicinity of the Fermi energy. The diagram underneath depicts the relevant spin configurations: the outer vertical arrows refer to the magnetization of external electrodes, whereas the inner ones refer to the magnetization of extra magnetic monolayers (the rectangle symbolizes the SWCNT). The horizontal large arrow symbolizes the transition to the parallel, i.e. saturated, configuration. The parameters generating up-oriented magnetic moments are: $\epsilon_{\text{electrode}\uparrow} = \epsilon_{\text{mono}\uparrow} = -2.32$ and $\epsilon_{\text{electrode}\downarrow} = \epsilon_{\text{mono}\downarrow} = 1.6$ (the moments get flipped upon the interchange $\epsilon_\uparrow \Longleftrightarrow \epsilon_\downarrow$).

transition oxide layer on top of the transition metal electrode. The exchange coupling of the electrode/oxide-monolayer layer is assumed to be antiferromagnetic and reduced in magnitude (implying $t_c = -0.35$), whereas the magnetic moment of the monolayer is enhanced up to $P_{\text{mono}} = 75\%$. Under such conditions the GMR approaches its maximum value of 100%. It is noteworthy that all the presented conductance spectra reflect in many respects the 'fingerprints' of the nanotubes:

(i) The spectra are cut-off to the width of up to $6|t|$, as in the pristine SWCNT, although the detached electrodes in our model have got an energy bandwidth equal to $16|t|$.

(ii) The dominant peaks close to the Fermi energy are separated from one another by $hv_F/(2L)$ (about 0.125 for $L = 20.5$ in the present units).

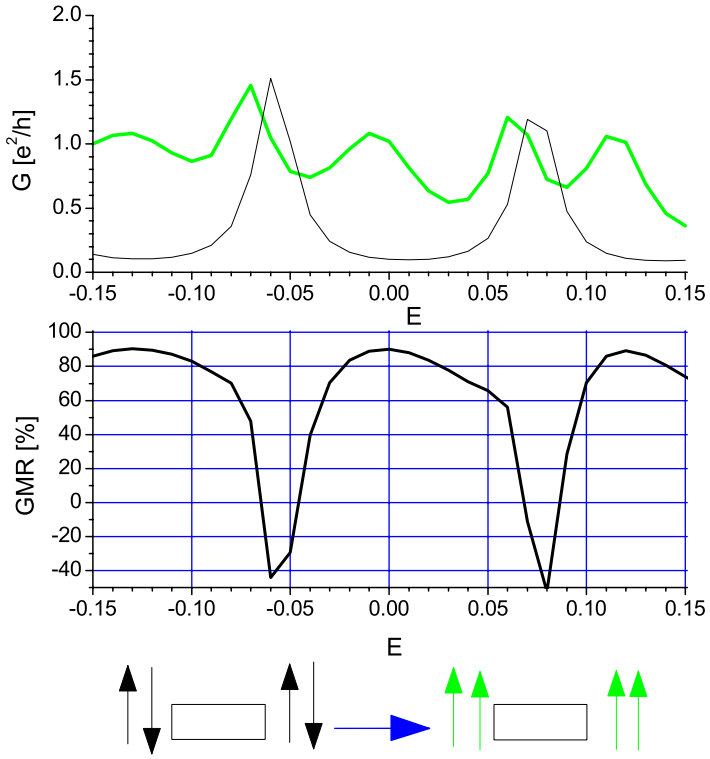

Figure 4. As figure 3 but now the thin curve in the upper panel applies to the antiferromagnetic coupling between the electrodes and the monolayers (see the lhs of the diagram). In this case the energy band mismatch in the interface regions is enhanced, leading to a significant reduction of the conductance in the non-saturated configuration. The parameters are: $\epsilon_{\text{electrode}\uparrow} = \epsilon_{\text{mono}\uparrow} = -2.32$, $\epsilon_{\text{electrode}\downarrow} = \epsilon_{\text{mono}\downarrow} = 1.6$ and $t_c = -1$.

On symmetry grounds, in the configurations '↑↑↓↓' and '↑↓↑↓' there is no conductance peak splitting, whereas in the saturated case '↑↑↑↑' the electron contributions to the conductance are spin-dependent and the splitting occurs (unless the suppressed spin channel nearly completely vanishes as in figure 5). In some cases, quite a small change in the Fermi position can lead to huge changes in the GMR. So there appears a possibility of tuning the GMR value by means of the gate voltage.

4. Conclusions

A Coulomb-blockade-free transport has been considered, so the results may be related to experiments performed at a fixed gate voltage which drives the system beyond the blockade regime. We find the typical resistance is much lower than 1 MΩ (conductance much greater than $0.02e^2/h$), except for the case of the suppressed channel transport, when the antiparallel alignment of the electrodes coincides with the antiferromagnetic exchange coupled electrode/monolayer interfaces. In the latter case, tunnel-like contacts are formed for the electron transport.

It has been shown that the existence of an additional magnetic monolayer on magnetic electrodes critically influences the giant magnetoresistance. In the case when the monolayer has

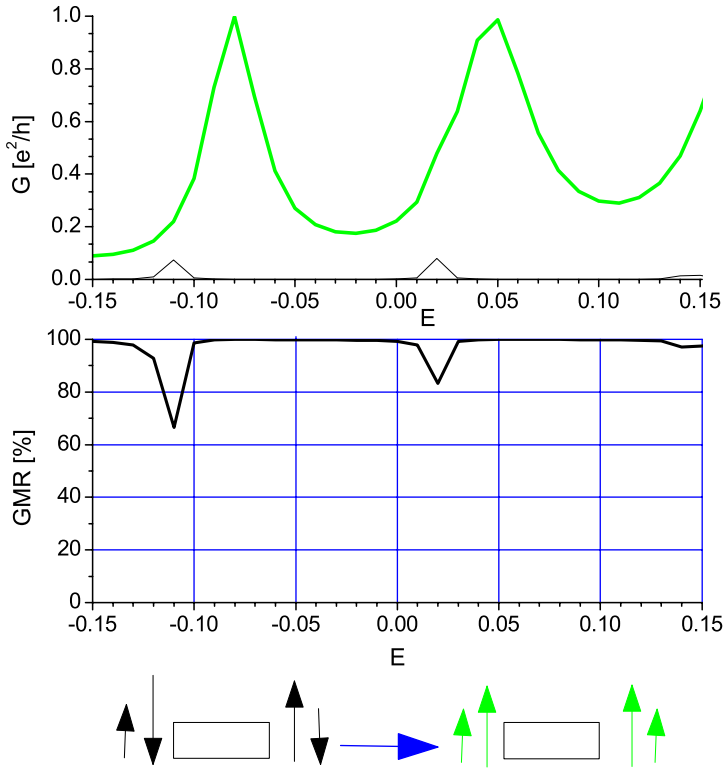

Figure 5. As figure 4 but now the antiferromagnetically coupled adjacent magnetic layers have different magnetizations (50% and 75%, respectively). The more and more increased energy band mismatch results in the complete suppression of conductance in the non-saturated configuration. The modified parameters are: $\epsilon_{\text{mono}\uparrow} = -2.93$, $\epsilon_{\text{mono}\downarrow} = 3.86$ and $t_c = -0.35$.

an enhanced magnetic moment the GMR value can approach 100%, i.e. both the spin-dependent conductance channels may become blocked in the anti-aligned-electrode configuration. Our computations show that this scenario can be realized provided that the extra monolayer has got a magnetic moment oriented antiparallel to the magnetization of the adjacent electrode. It is noteworthy that, in contrast to the half-metallic electrodes case, for this phenomenon to occur none of the spin-dependent local density of states has to vanish at the electrode surfaces. So the SWCNT, together with the adjusting monolayers, act as a spin filter which hardly lets through electrons which, due to the strong confinement (band mismatch), behave as if they were localized. Our computations also show that the GMR value depends in a sensitive way on the chemical potential position. These findings shed more light on the apparently poor reproducibility of experimental results on the GMR effect in ferromagnetically contacted SWCNTs. It appears that the above-mentioned problems originate from insufficient control of conditions at the ferromagnetic electrodes.

Acknowledgments

I thank Gerd Schön, Carlos Cuevas and Jan Martinek for fruitful discussions. The DAAD Foundation and the KBN (research project PBZ-KBN-044/P03-2001) as well as the EU Centre of Excellence (contract G5MA-2002-04049) are also acknowledged.

References

[1] Damle P S, Gosh A W and Datta S 2001 *Phys. Rev.* B **64** 201403
[2] Emberly E G and Kirczenow G 1998 *Phys. Rev.* B **58** 10911
[3] Heurich J, Cuevas J C, Wenzel W and Schön G 2002 *Phys. Rev. Lett.* **88** 256803
[4] Schulz M 1999 *Nature* **399** 729
[5] Dekker C 1999 *Phys. Today* (May) 22
[6] McEuen P L 2000 *Phys. World* **13** 21
[7] Tsukagoshi K, Alphenaar B A and Ago H 1999 *Nature* **401** 572
[8] Zhao B, Mönch I, Mühl T and Schneider C M 2002 *Appl. Phys. Lett.* **80** 3144
[9] Jensen A, Nygård J and Borggreen J 2003 Toward the controllable quantum states *Proc. Int. Symp. on Mesoscopic Superconductivity and Spintronics* ed H Takayanagi and J Nitta (Singapore: World Scientific) pp 33–7
[10] Kim J, Kim J-R, Park J W, Kim J-J, Kang K, Kim N and Woo B-C 2002 *23rd Int. Conf. on Low Temperature Physics (Aug. 2002)*
[11] Mehrez H, Taylor J, Guo H, Wang J and Roland C 2000 *Phys. Rev.* B **84** 2682
[12] Krompiewski S 2003 *Phys. Status Solidi* a **196** 29
[13] Krompiewski S 2003 *ICM'03 Proc.*; *J. Magn. Magn. Mater.* at press
[14] Anisimov V I, Zaanen J and Andersen O K 1991 *Phys. Rev.* B **44** 943
[15] Damle P, Rakshi T, Laulsson M and Datta S 2002 *Preprint* cond-mat/0206328
[16] Krompiewski S, Martinek J and Barnaś J 2002 *Phys. Rev.* B **66** 073412
[17] Todrov T N *et al* 1993 *J. Phys.: Condens. Matter* **5** 2389
[18] Cunningham S L 1974 *Phys. Rev.* B **10** 4988
[19] Schulthess T C and Butler W H 1998 *Phys. Rev. Lett.* **81** 4516
[20] Yaliraki S N, Kemp M and Ratner M A 1999 *J. Am. Chem. Soc.* **121** 3428
[21] Wildöer J W G, Venema L C, Rinzler A G, Lemay S G, Janssen J W, Smalley R E and Dekker C 1998 *Nature* **391** 59
[22] Venema L C, Janssen J W, Buitelaar M R, Wildöer J W G, Lemay S G, Kouwenhoven P P and Dekker C 2000 *Phys. Rev.* B **62** 5238
[23] Lemay S G, Janssen J W, van den Hout M, Mooij M, Bonikowski M J, Willis P A, Smalley R E, Kouwenhoven P P and Dekker C 2001 *Nature* **412** 617